Impaired CMV immunity in idiopathic pulmonary fibrosis lung transplant recipients with short telomeres

Iulia Popescu, Hannah Mannem, Spencer A. Winters, Aki Hoji, Fernanda Silveira, Emily McNally, Matthew R. Pipeling, Elizabeth A. Lendermon, Matthew R. Morrell, Joseph M. Pilewski, Vidya Sagar Hanumanthu, Yingze Zhang, Swati Gulati, Pali D. Shah, Carlo J. Iasella, Christopher R. Ensor, Mary Armanios and John F. McDyer

ONLINE DATA SUPPLEMENT

SUPPLEMENTAL MATERIALS AND METHODS

PBMC Samples and Antigen Re-stimulation

Blood samples from LTRs were obtained within 5-14 days of detection of *de novo* viremia (acute primary CMV infection) in D+R- LTRs. For D+R+ LTRs, samples were obtained during viremic episodes in relapsers or non-viremic time points in controllers after discontinuation of antiviral prophylaxis. PBMC were isolated from heparinized blood samples by density gradient centrifugation using Ficoll-Paque (GE Healthcare) and cryopreserved in liquid nitrogen (Taylor Wharton) until use. Single-pools of overlapping 15-mer peptides for pp65 (JPT) were used for PBMC re-stimulation. PBMC were cultured in round-bottom tissue culture tubes (Sarstedt) in the presence or absence (medium alone) of pooled pp65 peptides or Staphylococcus enterotoxin B at (1μg/mL). All stimulations for intracellular cytokine staining (ICS) were performed using 10^6 cells per condition for 6 hours at 37°C with brefeldin-A (10 μ/mL) (Sigma) added for the final 4 hours of culture. Monensin (5 μg/mL) along with brefeldin-A and anti-CD107a-Pacific Blue (Pac Blue) was added at the beginning of culture when CD107a was measured. All cells were collected for flow cytometric analysis with a range of $0.5\text{-}1x10^6$ total events collected per condition. All gates for cytokine frequencies were set using the medium alone control and subtracted from peptide re-stimulated samples frequencies. In certain proliferation experiments, cells were cultured for 6 days, and labeled with CFSE (0.2 μM; Invitrogen) to determine proliferation. Cell cultures were harvested at day 6, washed, rested overnight in medium alone, and secondary re-stimulation performed in the presence or absence of CMV-pp65 peptides for 6h (similar to primary cultures) and assessed for proliferation via CFSE dilution and cytokine by ICS.

Flow cytometry

Following in vitro re-stimulation, cells were surface-stained with fluorochrome-labeled antibodies anti-CD3-Alexa-Fluor700, anti-CD8-V500 and anti-CD4-APCCy7 (BD Biosciences). Live/Dead Fixable Blue Dead-Cell Stain (Invitrogen) was used for gating on viable cells. Cytofix/ Cytoperm (BD Biosciences) reagents were used to fix and permeabilize cells for ICS using anti-IFN-γ-BV605, anti-TNF-α-PE-Cy7, anti-IL-2-BV650, anti-Granzyme B-PE CF 594, anti-CD107a-Pacific Blue (BD Biosciences). Cell fluorescence was analyzed using a custom LSR Fortessa cytometer equipped with a UV Laser (BD Biosciences). Flow cytometry data were analyzed using FlowJo software (Tree Star).

Telomere length measurement

Telomere length was measured on PBMCs by flow cytometry and fluorescence in situ hybridization as previously described (1, 2). Each patient sample was plotted relative to a validated age-adjusted nomogram derived from healthy controls (3). The delta lymphocyte telomere length was calculated as the difference from the age-adjusted median in kb as previously described (4).

DNA sequencing and analysis

DNA was extracted from frozen PBMCs using the Gentra Puregene Kit B (Qiagen). We designed primers to sequence the seven known familial pulmonary fibrosis telomere genes plus SFTPC using the TruSeq Custom Amplicon Low Input Kit (Illumina) as previously described (5). Amplicons targeted the coding regions and intron-exon junctions of *TERT* (NM_198253.2),

TR (NR_001566.1), *RTEL1* (NM_001283009.1), *PARN* (NM_002582.3), *DKC1* (NM_001363.3), exon 6 of *TINF2* (NM_012461.2), *NAF1* (NM_138386.2) and *SFTPC* (NM_003018.3) using the online Design Studio software (Illumina). Sequencing was performed on an Ilumina MiSeq sequencer.

Analysis of sequence data and verification

To identify ultra-rare, potentially pathogenic variants, we examined variants that were covered at least at 8x depth and filtered out common variants [defined as present in dbSNP build 131, Phase 1 of the 1000 Genomes Projects, or that were found at a greater than 0.001 minor allele frequency in the Exome Variant Server (http://evs.gs.washington.edu/EVS) or the Exome Aggregation Consortium browser (http://exac.broadinstitute.org)] as previously described (5, 6). The databases were accessed on November 1, 2017. Heterozygous autosomal variants were required to be present in at least a third of the reads while *DKC1* variants (on the X-chromosome) had to be called homozygous by the GATK pipeline in male cases. Variants were deemed pathogenic if they were previously implicated in disease or were obviously deleterious to protein function (i.e. frameshift, nonsense, canonical splice altering). Ultra-rare variants that were associated with short telomere length ($\leq$ 10th percentile) but had unclear consequences on protein function were deemed likely pathogenic. Variants that fell outside the known pathogenic hotspots were deemed benign and remaining variants were annotated as variants of unknown significance. Table 2 includes the prevalence of rare variants in the Genome Aggregation Database (gnomAD) accessed on January 15, 2018.

Statistical Analysis

Statistical analysis was performed using Graph Pad Prism (California) and SPSS version 22. Fisher's exact test was utilized to test significance of categorical data. As no assumption was made regarding the Gaussian distribution of measured continuous variables, the non-parametric tests of Wilcoxon signed-rank, Mann-Whitney U, and Spearman's rank correlation coefficient were also used. Additionally, Kaplan-Meier survival analysis and Cox-proportional hazards modeling controlling for Valganciclovir were performed to assess time to relapse. Multifunctional analysis and presentation of distributions was performed using SPICE software(7), downloaded from http://exon.niaid.nih.gov/spice version 5.1. A two-tailed P value of < 0.05 was considered statistically significant.

REFERENCES

1. Baerlocher GM, Vulto I, de Jong G, Lansdorp PM. Flow cytometry and fish to measure the average length of telomeres (flow fish). *Nat Protoc* 2006;1:2365-2376.

2. Alder JK, Hanumanthu VS, Strong MA, DeZern AE, Stanley SE, Takemoto CM, Danilova L, Applegate CD, Bolton SG, Mohr DW, Brodsky RA, Casella JF, Greider CW, Jackson JB, Armanios M. Diagnostic utility of telomere length testing in a hospital-based setting. *Proceedings of the National Academy of Sciences* 2018;115:E2358-E2365.

3. Stanley SE, Gable DL, Wagner CL, Carlile TM, Hanumanthu VS, Podlevsky JD, Khalil SE, DeZern AE, Rojas-Duran MF, Applegate CD, Alder JK, Parry EM, Gilbert WV, Armanios M. Loss-of-function mutations in the rna biogenesis factor naf1 predispose to pulmonary fibrosis-emphysema. *Sci Transl Med* 2016;8:351ra107.

4. Alder JK, Chen JJ, Lancaster L, Danoff S, Su SC, Cogan JD, Vulto I, Xie M, Qi X, Tuder RM, Phillips JA, 3rd, Lansdorp PM, Loyd JE, Armanios MY. Short telomeres are a risk factor

for idiopathic pulmonary fibrosis. *Proceedings of the National Academy of Sciences of the United States of America* 2008;105:13051-13056.

5. Stanley SE, Chen JJ, Podlevsky JD, Alder JK, Hansel NN, Mathias RA, Qi X, Rafaels NM, Wise RA, Silverman EK, Barnes KC, Armanios M. Telomerase mutations in smokers with severe emphysema. *The Journal of clinical investigation* 2015;125:563-570.

6. Parry EM, Gable DL, Stanley SE, Khalil SE, Antonescu V, Florea L, Armanios M. Germline mutations in DNA repair genes in lung adenocarcinoma. *J Thorac Oncol* 2017;12:1673-1678.

7. Roederer M, Nozzi JL, Nason MC. Spice: Exploration and analysis of post-cytometric complex multivariate datasets. *Cytometry Part A : the journal of the International Society for Analytical Cytology* 2011;79:167-174.

SUPPLEMENTAL FIGURE LEGENDS

Figure E1. IPF-TRs have increased risk of infectious complications due to CMV-infection, with no differences by CMV-serostatus. Compilation of CMV Complication-Score comparing IPF-LTRs with non-IPF-LTRs (*A).* Individuals receive 1 point for each i) relapsing viremia episode, ii) biopsy proven end-organ disease episode (pneumonitis, gastritis, or colitis), or iii) ganciclovir CMV-resistance. Results show a higher score for IPF-LTRs versus non-IPF-LTRs (p=0.02). *(B)* There is no difference in CMV-complications between D+/R-IPF-LTRs and D+/R+IPF-LTRs, nor between D+R-non-IPF-LTRs and D+R+non-IPF-LTRs. Statistical analysis performed using Mann-Whitney U-test with a two-sided P value of < 0.05 considered statistically significant.

Figure E2. Impaired CMV-specific $CD4^+$ T-cell effector responses and granzyme B loading capacity in IPF-LTRs with short telomere length ($TL \leq 10^{th}$ percentile). Pooled data of intracellular cytokine staining at 6 h for CMV pp65-specific $CD4^+$ T-cell function during acute CMV-infection. Values represent cell frequencies following re-stimulation with pp65 peptides minus medium alone (unstimulated) of $IFN\gamma^+$ *(A)*, $TNF\alpha^+$ *(B)*, $CD107a^+$ *(C)*, and $IL\text{-}2^+$ *(D)* from a subset of 31 LTRs. Also indicated are Controllers (C) (*blue dots*) versus Relapsers (R) (*red dots*) status. Pooled frequencies of $CD8^+GrzB^+$ (unstimulated PBMC) *(E)* from the same patients. Bars represent median values and *p*-values were calculated using the Mann-Whitney-Wilcoxon test.

Figure E3. D+R- IPF-LTRs demonstrate significantly reduced $CD8^+T\text{-}bet^+$ levels and $CD8^+$ CMV-specific proliferative responses. Pooled data showing the *ex vivo* $CD8^+T\text{-}bet^+$ frequencies *(A)* and cumulative data showing $CD8^+$ CMV pp65-specific proliferation at 6 days using CFSE

dilution *(B).* Also indicated are Controllers (C) (*blue dots*) versus Relapsers (R) (*red dots*) status. Both $CD8^+$T-bet^+ levels (*A*) and $CD8^+$ CMV-specific proliferative responses (*B*) did not differ by CMV-serostatus with IPF-LTRs. D+R-IPF-LTRs demonstrated significantly reduced $CD8^+$T-bet^+ levels and $CD8^+$ CMV-specific proliferative responses compared to age-matched D+R- non-IPF-LTRs Bars represent median values and *p*-values were calculated using the Mann–Whitney-Wilcoxon test with a two-sided P value of < 0.05 considered statistically significant.

Figure E4. Impaired SEB reactive T-cell effector responses and granzyme B loading capacity in IPF-LTRs with short telomere length (TL$\leq$10th percentile). Pooled data showing the frequencies of SEB-reactive $CD8^+$ *(left panel)* and $CD4^+$ *(right panel)* T-cell proliferative responses during acute CMV-infection from a total of 31 patients *(A)*. Pooled data of intracellular cytokine staining at 6 h for SEB-reactive $CD8^+$ T cell function during acute CMV-infection. Values represent cell frequencies following re-stimulation with SEB minus medium alone (unstimulated) of IFNγ^+ *(B),* TNFα^+ *(C),* $CD107a^+$ *(D)* from a subset of 31 LTRs. Also indicated are Controllers (C) (*blue dots*) versus Relapsers (R) (*red dots*) status. Bars represent median values and P-values were calculated using the Mann-Whitney-Wilcoxon test.

Figure E5. CMV pp65-specific $CD8^+$ effector responses, granzyme B and T-bet levels during active CMV differentiate the capacity for viral control in high-risk LTRs. Pooled data showing the CMV pp65-specific frequencies of $CD8^+$IFNγ^+ *(A),* $CD8^+$TNFα^+ *(B),* $CD8^+CD107a^+$ *(C),* $CD8^+$GrzB$^+$ *(D),* $CD8^+$T-bet^+ *(E),* and CMV pp65-specific $CD8^+$proliferative responses at day 6 by CFSE dilution among *(F)* among Relapsers (*red circles*) versus Controllers (*blue circles*)

during acute CMV-infection. Bars represent median values and P-value determined using the Mann-Whitney-Wilcoxon test.

Figure E1

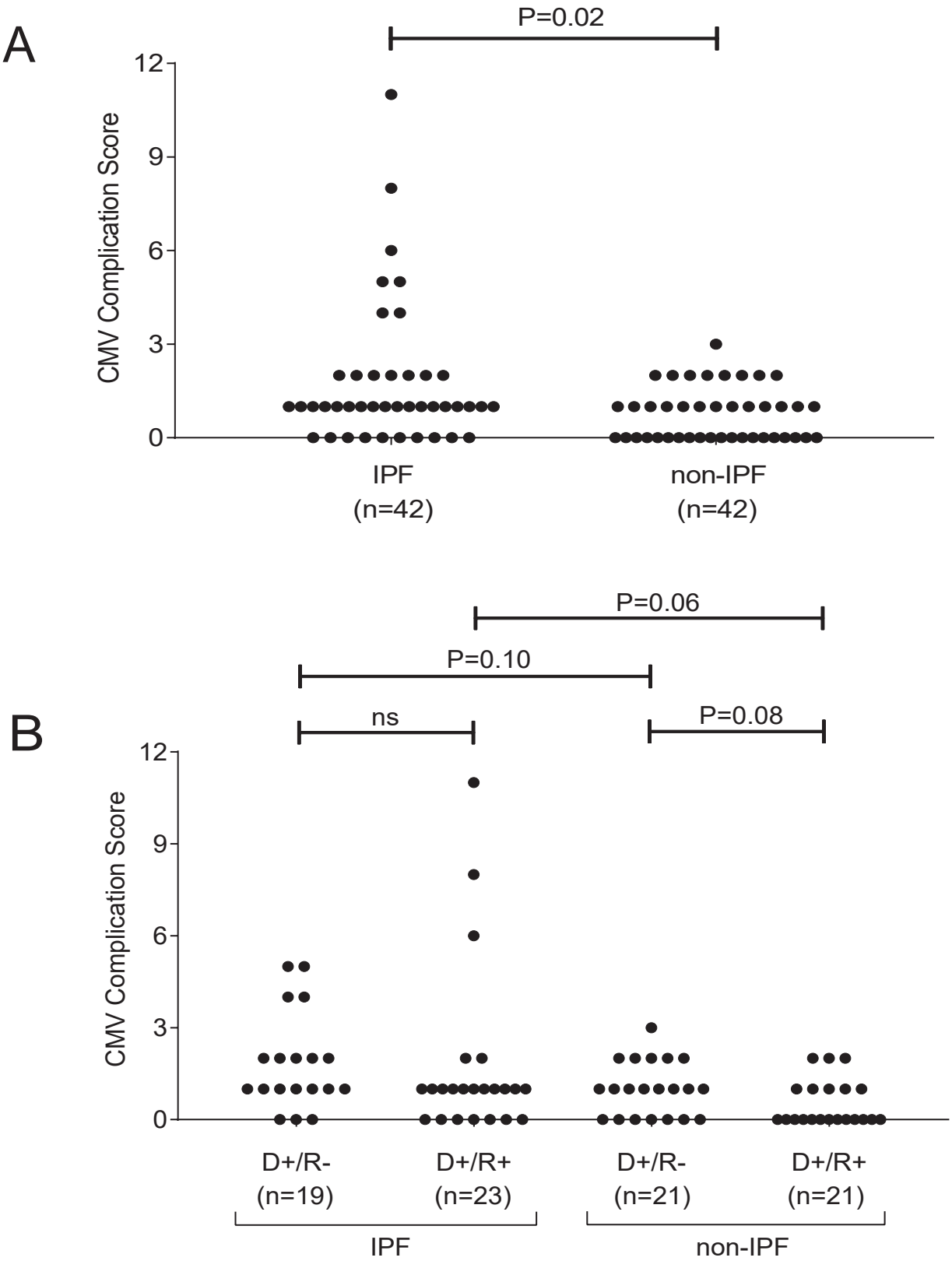
A
P=0.02
CMV Complication Score
12
9
6
3
0
IPF
(n=42)
non-IPF
(n=42)
B
P=0.06
P=0.10
ns
P=0.08
CMV Complication Score
12
9
6
3
0
D+/R-
(n=19)
D+/R+
(n=23)
D+/R-
(n=21)
D+/R+
(n=21)
IPF
non-IPF

Figure E2

Lorem ipsum

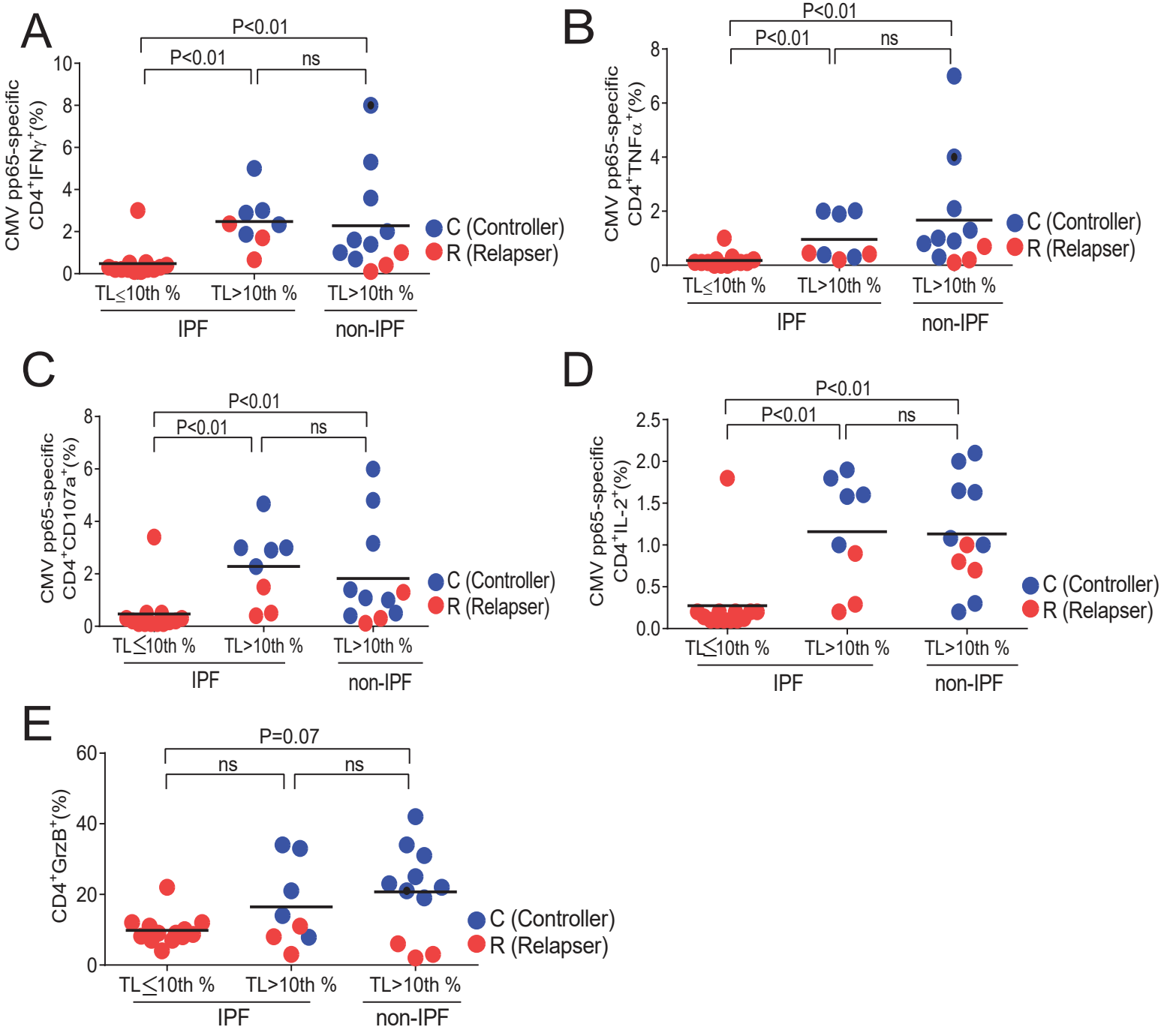

Figure E3

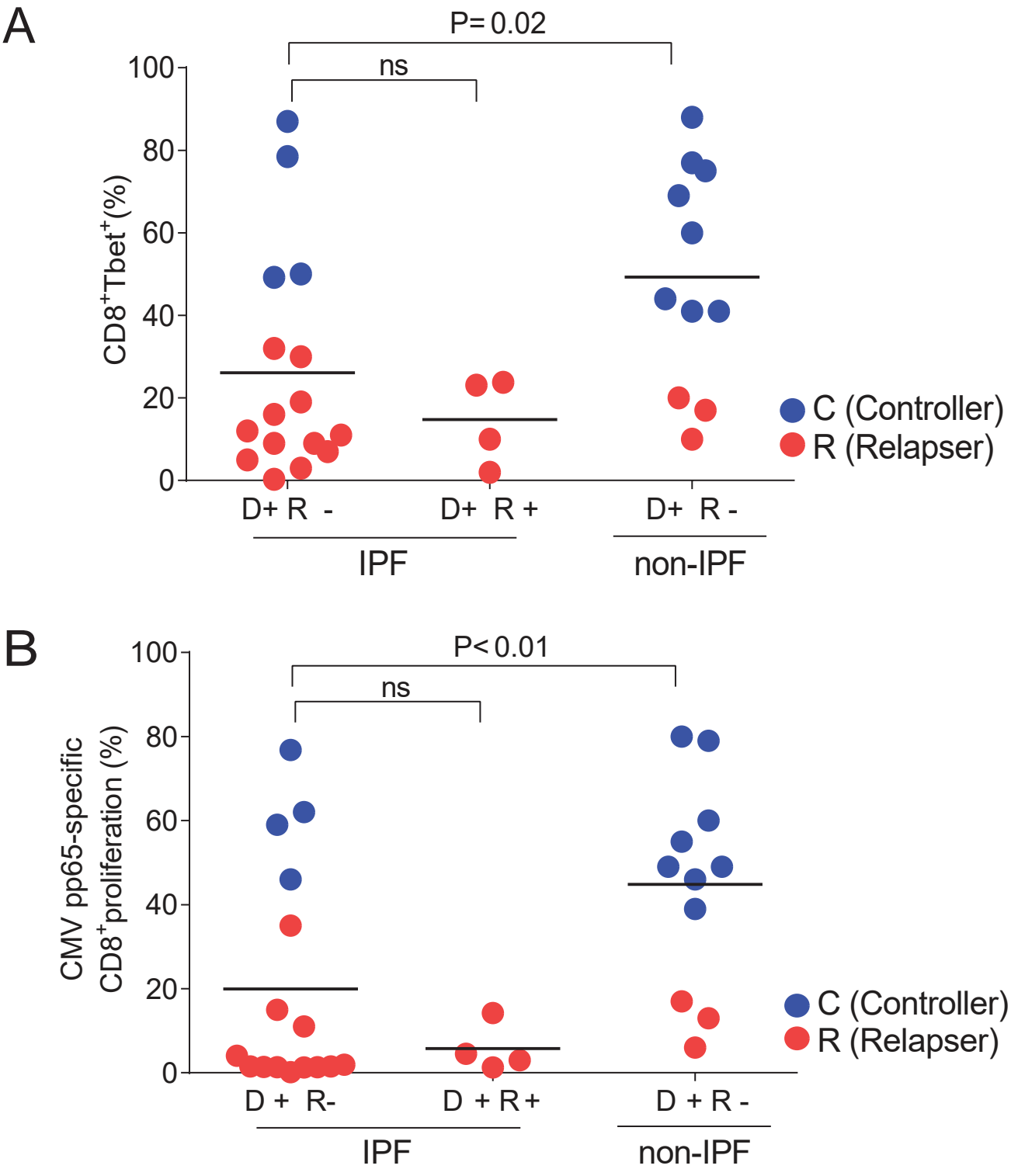
A
P= 0.02
ns
100
80
60
40
20
0
CD8+Tbet+(%)
D+ R -
D+ R +
D+ R -
IPF
non-IPF
C (Controller)
R (Relapser)
B
P< 0.01
ns
100
80
60
40
20
0
CMV pp65-specific
CD8+proliferation (%)
D + R-
D + R +
D + R -
IPF
non-IPF
C (Controller)
R (Relapser)

Figure E4

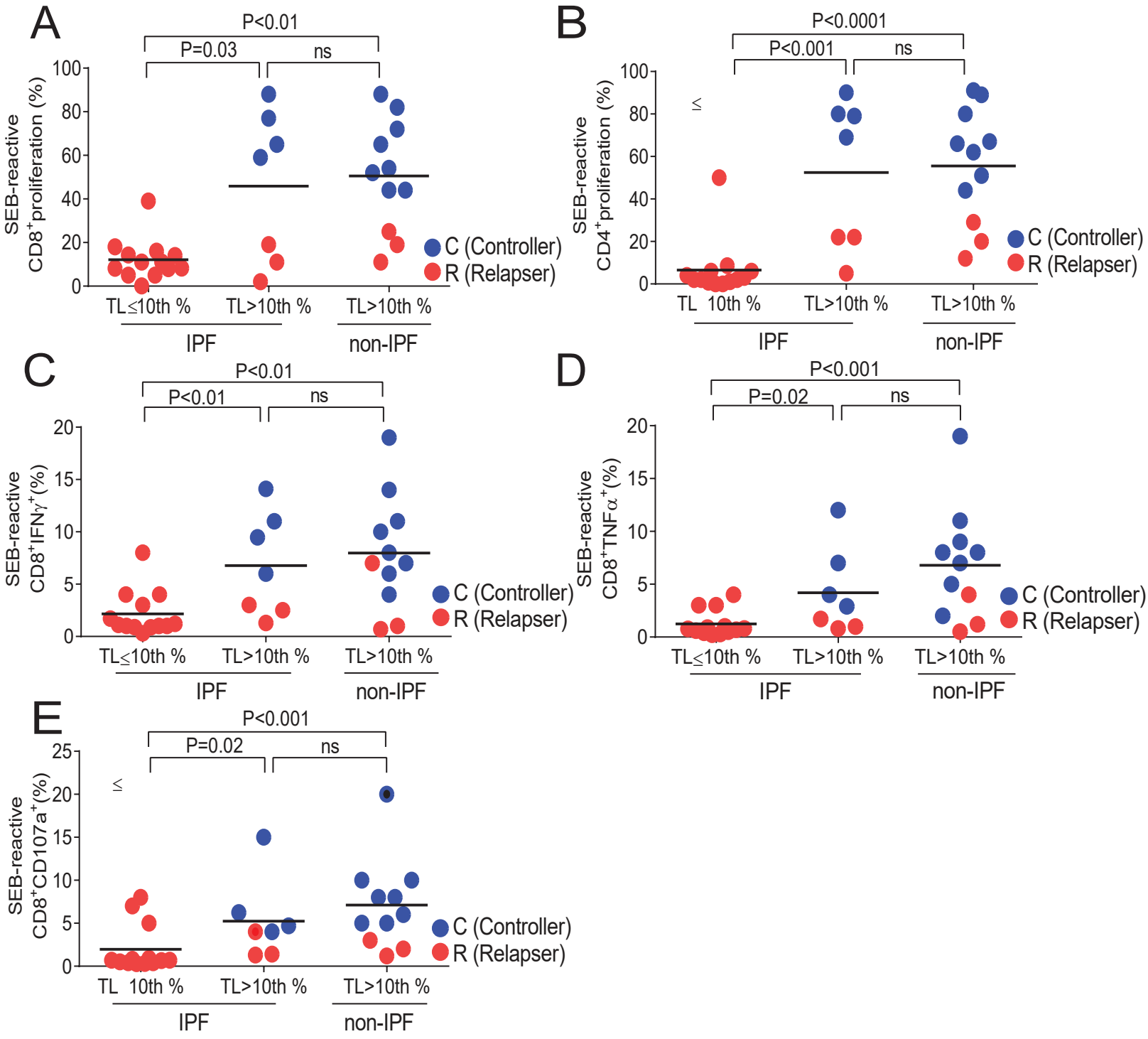
A
P<0.01
P=0.03
ns
SEB-reactive CD8+proliferation (%)
100
80
60
40
20
0
C (Controller)
R (Relapser)
TL≤10th %
TL>10th %
TL>10th %
IPF
non-IPF
B
P<0.0001
P<0.001
ns
SEB-reactive CD4+proliferation (%)
≤
TL 10th %
TL>10th %
TL>10th %
IPF
non-IPF
C (Controller)
R (Relapser)
C
P<0.01
P<0.01
ns
SEB-reactive CD8+IFNγ+(%)
20
15
10
5
0
TL≤10th %
TL>10th %
TL>10th %
IPF
non-IPF
C (Controller)
R (Relapser)
D
P<0.001
P=0.02
ns
SEB-reactive CD8+TNFα+(%)
20
15
10
5
0
TL≤10th %
TL>10th %
TL>10th %
IPF
non-IPF
C (Controller)
R (Relapser)
E
P<0.001
P=0.02
ns
SEB-reactive CD8+CD107a+(%)
≤
25
20
15
10
5
0
TL 10th %
TL>10th %
TL>10th %
IPF
non-IPF
C (Controller)
R (Relapser)

Figure E5

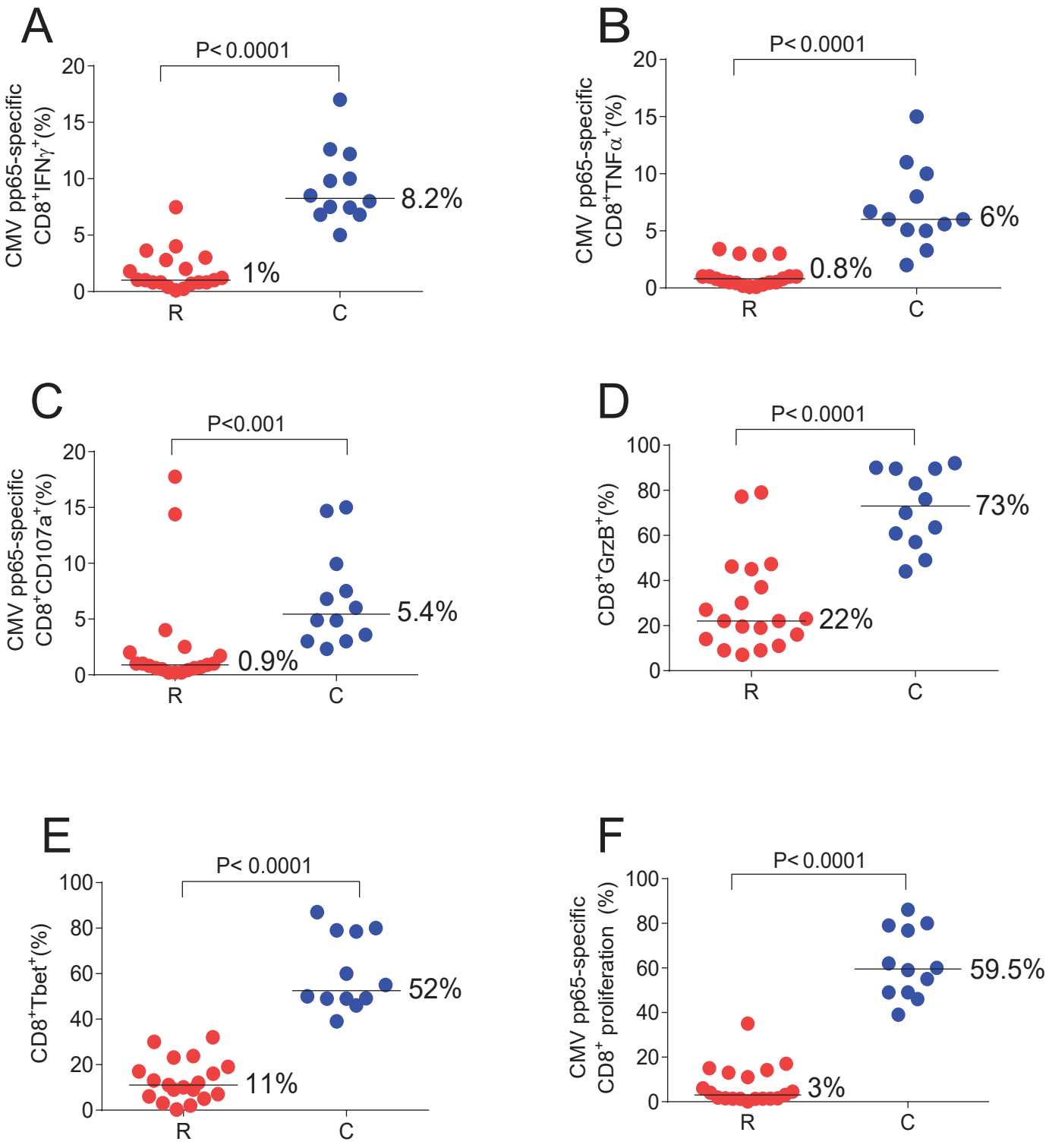
A
P< 0.0001
CMV pp65-specific CD8+IFNγ+(%)
20
15
10
5
0
8.2%
1%
R
C
B
P< 0.0001
CMV pp65-specific CD8+TNFα+(%)
20
15
10
5
0
6%
0.8%
R
C
C
P<0.001
CMV pp65-specific CD8+CD107a+(%)
20
15
10
5
0
5.4%
0.9%
R
C
D
P< 0.0001
CD8+GrzB+(%)
100
80
60
40
20
0
73%
22%
R
C
E
P< 0.0001
CD8+Tbet+(%)
100
80
60
40
20
0
52%
11%
R
C
F
P< 0.0001
CMV pp65-specific CD8+ proliferation (%)
100
80
60
40
20
0
59.5%
3%
R
C